Measurement: Sensors 10-12 (2020) 100021

Contents lists available at ScienceDirect

Measurement: Sensors

journal homepage: www.journals.elsevier.com/measurement

Mass flow rate measurement of solids in a pneumatic conveying pipeline in different orientations

Faisal Abbas, Lijuan Wang *, Yong Yan

School of Engineering and Digital Arts, University of Kent, Canterbury, Kent, CT2 7NT, UK

ARTICLE INFO

Keywords:
Pneumatic conveying
Gas-solid two-phase flow
Mass flow rate
Pipe orientation
Support vector machine
Partial mutual information
Firefly algorithm

ABSTRACT

Extensive work has been undertaken for the mass flow rate measurement of solids in a horizontal or vertical pneumatic conveying pipe. However, flow regime of the two-phase flow is highly influenced by different orientations of the pipe, resulting in different characteristics of sensor signals and hence large errors in mass flow rate measurement using conventional methods. This paper presents a novel technique to measure the mass flow rate of pneumatically conveyed particles in different pipe orientations. A range of low-cost sensors, including an array of electrostatic sensors, a differential-pressure transducer, and an accelerometer, are integrated to form a sensing unit. Data-driven models, based on support vector machine (SVM), are developed to take the selected features from post-processed sensor data and infer the mass flow rate of solids in different pipe orientations. The partial mutual information algorithm is applied to quantify the importance of each feature. The firefly algorithm is used to optimize the selection of useful features and tune the learning parameters in SVM models. Experimental tests were conducted on a pneumatic conveying test rig circulating flour over the mass flow rate of solids from 3.2 g/s to 35.8 g/s in pipe orientations from 0° to 90°. Performance comparisons are made between the conventional SVM model and the optimised SVM models with the training data from horizontal orientation and different orientations, respectively. Results demonstrate that the relative error and repeatability of the measured mass flow rate of solids with the optimized SVM model are both improved to within ±12%.

1. Introduction

Mass flow rate measurement of pneumatically conveyed solids in power, cement, and food industries remains one of the primary technical problems confronted by the operators. An online continuous and non-invasive measurement system is desirable to monitor the flow conditions, avoid pipe blockage, and maximise the process efficiency. Over the past few years, a variety of sensing principles, including electrostatic [1], ultrasonic [2], capacitive [3], acoustic [4], optical [5] sensors and nuclear magnetic resonance [6], have been applied to measure the velocity, concentration and mass flow rate of particles in horizontal or vertical pipes. Amongst all of these sensor paradigms, electrostatic sensors perform well in terms of robustness in a hostile environment, non-intrusiveness in service, low cost, and low maintenance requirements. However, the measurement of suspension density (concentration) and mass flow rate of solids in two-phase flow is still challenging through direct measurement techniques based on the traditional sensors [7].

In order to directly obtain the mass flow rate, advanced data-driven modelling based on machine learning techniques has been attempted as an effective approach [7,8]. Although some research has been undertaken to measure the concentration of solids in two-phase flow or identify the flow regime using electrostatic sensors and machine learning algorithms, there is still limited research on mass flow rate measurement of solids through multi-modal sensing and data-driven modelling. Wang et al. [9] integrated capacitive and electrostatic sensors to measure the coal/biomass/air three-phase flow rate and developed an adaptive network based fuzzy inference system to infer the volumetric-concentration of each phase. Hu et al. [10] extracted three features from electrostatic signals and developed backpropagation neural networks to identify the flow regime of gas-solid two-phase flow in a horizontal pipe. Yan et al. [11] applied a single ring-shaped electrostatic sensor and a backpropagation neural network to measure the velocity and mass flow rate of pneumatically conveyed solids. Our recent research [12] investigated the performance of three different machine learning models including artificial neural network, support vector machine and convolutional neural network on the measurement of mass flow rate of solids in gas-solid two-phase flow. It turns out that SVM outperforms ANN and CNN in terms of measurement accuracy [12]. However, in the conventional SVM models, the model output is influenced by the model parameters, such as learning rate, regularization, and kernel

* Corresponding author.
E-mail address: L.Wang@kent.ac.uk (L. Wang).

https://doi.org/10.1016/j.measen.2020.100021
Received 31 July 2020; Received in revised form 1 October 2020; Accepted 5 October 2020
Available online 20 October 2020
2665-9174/© 2020 The Authors. Published by Elsevier Ltd. This is an open access article under the CC BY-NC-ND license (http://creativecommons.org/licenses/by-nc-nd/4.0/).

List of abbreviations

ANN	Artificial neural network
CNN	Convolutional neural network
DP	Differential pressure
FA	Firefly algorithm
NI DAQ	National Instrument Data Acquisition Device
PMI	Partial mutual information
PSD	Power spectral density
PSO	Particle swarm optimization
RBF	Radial basis function
RMS	Root mean square
SVM	Support vector machine
VFD	Variable frequency drive

parameters as well as the dimension of the input feature vector. Hence, an optimization algorithm is required to obtain the appropriate values for all the model parameters. Many researchers have integrated SVM with a variety of optimization algorithms, including grey wolf algorithm [13], brain storm optimization [14] and PSO [15,16] algorithms and applied them in different applications. A performance comparison between the FA, PSO, and artificial bee colony algorithm was undertaken for non-linear mathematical problems and it has been found out that the FA performs better than the others for a noisy non-linear optimization problem [17]. Therefore, the FA is used in this paper to optimise the SVM model parameters.

Previous research mostly focuses on the gas-solid flow measurement in horizontal or vertical pipes. However, the triboelectric charge and differential pressure in the pipe also depend on the pipe orientations. At tilted orientations, the solids hit with the walls of the bending pipe section, which can influence the energy and charge magnitude of particles. Moreover, pipe orientation may bring a change in gravitational force and momentum of the solids which can disturb the differential pressure across a pipe section. Tripathi et al. [18] investigated the total bend drop pressure in three orientations of the pipe, including horizontal-horizontal, horizontal-vertical, and vertical-horizontal in dilute phase conveying system. They have found out that the change in pressure drop was caused by the change in momentum in different orientations of the pipe. As limited research is carried out to measure the mass flow rate in different pipe orientations. Therefore, the effects of different pipe angles on the electrostatic sensor and DP transducer need to be investigated to produce the angle compensated mass flow rate measurement.

This paper proposes a novel method to measure the mass flow rate of solids in different orientations of a pipe using sensor fusion and optimized SVM models. The sensing unit includes electrostatic sensors, a DP transducer, and an accelerometer. The importance of all the statistically extracted features, presented in Refs. [12], is quantified using the PMI technique and then an optimal number of useful features is determined with the FA. SVM models are developed based on the training data and the FA is applied to optimize the parameters of SVM models to improve the accuracy of mass flow rate measurement. Experiments were conducted on a laboratory scale test rig in different pipe orientations in the range of 0–90°. The effectiveness of the proposed method is evaluated by comparing the results from the conventional and optimized SVM models which are trained with one as well as all pipe angles.

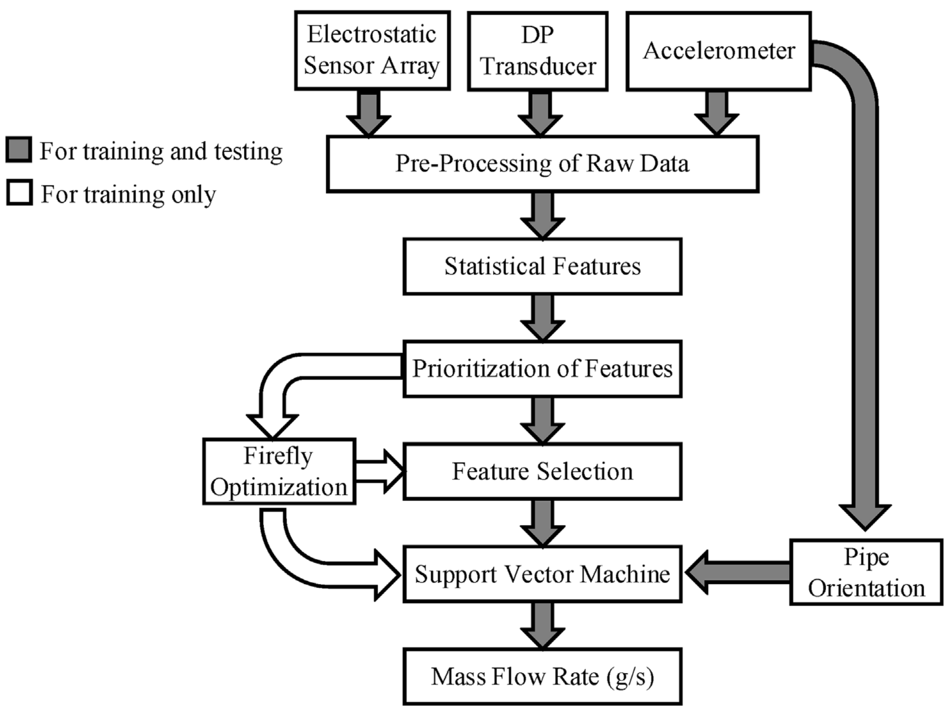

Fig. 1. Measurement strategy.

2. Methodology

2.1. Overall measurement strategy

The overall measurement strategy, as shown in Fig. 1, starts with the collection of raw data from the sensing unit which consists of an array of electrostatic sensors, a DP transducer, and an accelerometer. These three types of sensors are selected in order to acquire sufficient and complementary information about the physical characteristics of the flow (Section 2.2). During pneumatic transportation, solids are electrically charged due to triboelectric charging effect. Electrostatic sensors are used to sense the electrostatic charge and the amplitude of electrostatic signals is related to the velocity, concentration and hence mass flow rate of solids [1,19,20]. The differential pressure is the pressure difference between the inlet and outlet of a pipe section. It is directly related to the flow

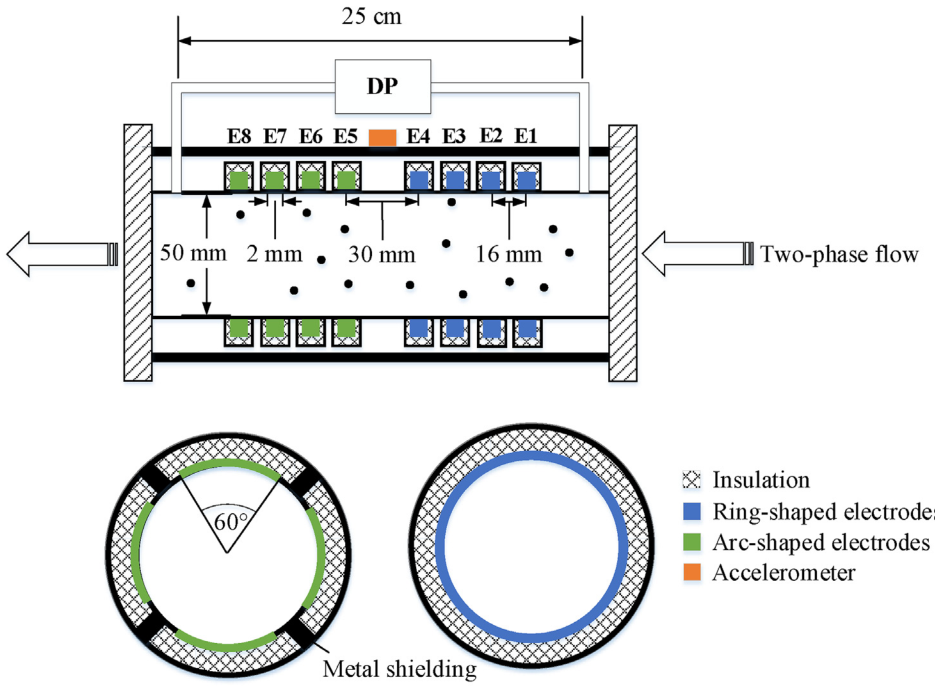

Fig. 2. Structure of the sensing unit.

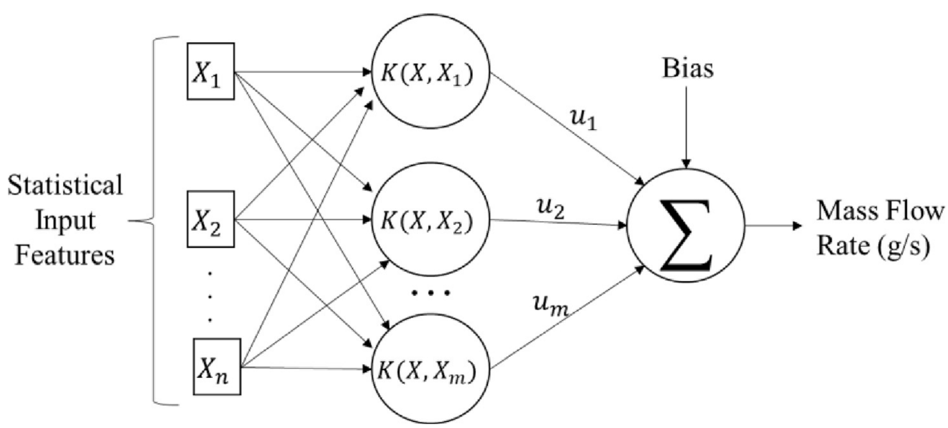

Fig. 3. Structure of SVM

velocity and solids concentration [19]. Therefore, the output of the DP transducer contains information about the mass flow rate of solids. The raw data needs to be segregated into the corresponding clusters of mass flow rate conditions. Unnecessary peaks and the glitches in the sensing data are removed at the stage of removal of outliers. All the possible statistical features, presented in the previous study [12], are extracted from all the smoothened and conditioned sensor data. The PMI is used to measure the information between each statistical feature and its corresponding output. Based on the values of PMI, each feature is prioritized by keeping the most useful features on the top. FA is used to optimize the selection of input features and the learning parameters of the SVM model including kernel scale, delta gradient tolerance, gap tolerance, and epsilon. All the arrows filled with a grey colour in Fig. 1 show the permanent connection between blocks. However, the shaded arrow connections in Fig. 1 show the temporary existence of the FA during the training process. Once the features are selected and the parameters of the model are optimized during the learning process, the developed SVM model will be directly used to infer the mass flow rate of solids.

2.2. Sensing unit

Fig. 2 shows the internal structure of the sensing unit used to carry out this research. When the particles travel in a pneumatic pipe, the electrostatic charge is generated due to the triboelectric effect of moving particles in the pipe. Therefore, electrostatic sensors can sense the level of charge on the particles, which is related to the concentration of solids. A set of four ring-shaped electrostatic sensors (E1, E2, E3 and E4) and a set of four arc-shaped electrostatic sensor arrays (E5, E6, E7 and E8) are combined to determine the localized and averaged charge values of particles, respectively. The fusion of multiple electrostatic sensors can increase the reliability of measurement and provide resilience to failure, e.g. a faulty sensor. The width and the thickness of all the electrodes are 2 mm and 3 mm, respectively. As the pressure drop across the test section is affected by the mass flow rate in different pipe orientations, a DP transducer is applied to measure the pressure difference across the pipe section. The accelerometer is installed on the pipe to record the information of different pipe orientations.

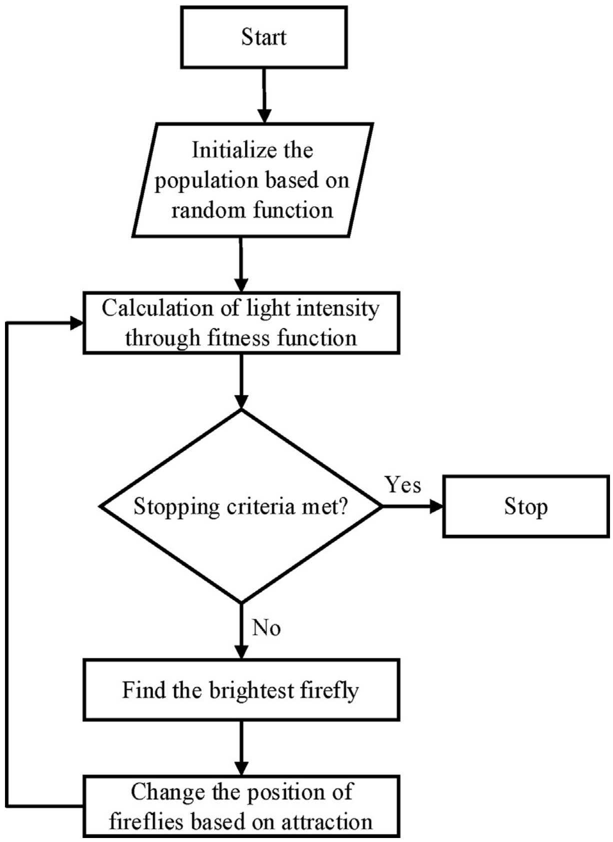

Fig. 4. Flow chart of FA.

2.3. Soft computing algorithms

The nature of the sensor signals becomes further complex when recorded in different orientations of pipe. Therefore, a data-driven model is required to establish the relationship between the input features and the mass flow rate of solids. Owing to the good generalisation ability and prediction accuracy, SVM is a more suitable data-driven model for gas-solid flow measurement [12]. Fig. 3 shows the typical structure of SVM model which is used in this research. Statistical features, optimally selected by PMI and FA (Section 4.4), are used as the inputs to the SVM model. The goal of the SVM model is to identify a hyperplane in an N-dimensional space with N number of features that classify the data points with the highest margins. Each node in the hidden layer converts the input data into another feature space using the kernel function. Compared with other kernel functions including linear, polynomial, and Gaussian, RBF is widely used in the domain of regression with better performance. The number of nodes in the hidden layer can be determined experimentally by the guidelines mentioned in Refs. [20]. In this paper, the internal parameters of the model, including kernel scale, delta gradient tolerance, gap tolerance and epsilon, are tuned to their optimal values using the firefly optimization algorithm (Section 4.4). In the process of SVM training, the algorithm divides the element of the predictor matrix by the value of the kernel scale. Then the appropriate kernel norm is applied to compute the gram matrix. Delta gradient tolerance defines the tolerance for the gradient difference between the upper and lower violators in the SVM solver and is used to set the threshold for optimization convergence. Gap tolerance is the threshold defined to maximize the location of the decision boundary. The whole training process is terminated as soon as the threshold reaches the value of gap tolerance. The value of epsilon defines the half width of epsilon-insensitive zone which influences the number of support vectors used to create the regression function [21]. The larger the epsilon, the smaller the support vectors selected. On the other hand, a higher epsilon value results in more flat estimates. The value of the epsilon evaluates the accuracy of the approximated function. It relies entirely on the target values for the training set. If the epsilon is larger than the target range, good accuracy in the predicted result cannot be achieved.

The performance of the conventional SVM model is sensitive to its parameters such as kernel scale, delta gradient tolerance, gap tolerance, and epsilon. Careful tuning of these parameters can significantly improve the prediction accuracy. Furthermore, a little change in the dimension of the input feature vector can significantly affect the tuning of these parameters. Therefore, an optimization algorithm is required to determine the best combination of all the parameters. Metaheuristic algorithms, influenced by the nature of many dynamic entities, play a critical role in modern global optimization algorithms, soft computing, and cognitive intelligence. Among the new metaheuristics, the FA is found to be very effective with multi-modal and global/local optimization issues. The FA was proposed by Yang in 2008 [22]. This algorithm adapted the behaviour of firefly swarms to build a multi-optimal functional optimization algorithm. In particular, it used the idea of how the light of the individual fireflies merged them and a randomness factor to facilitate the discovery of the solution space. Fig. 4 shows the steps involved in the implementation of the FA while integrated with the proposed methodology.

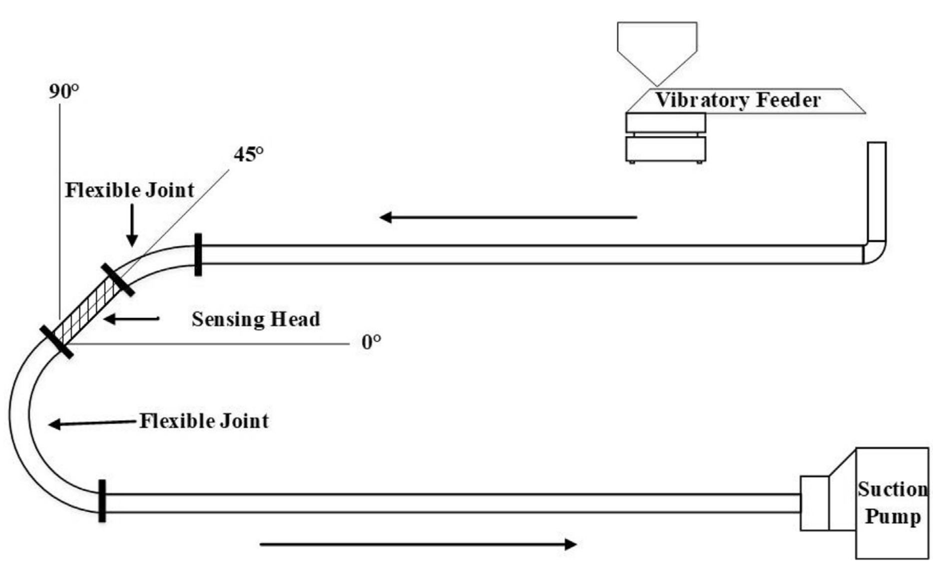

Fig. 5. Schematic of the test rig.

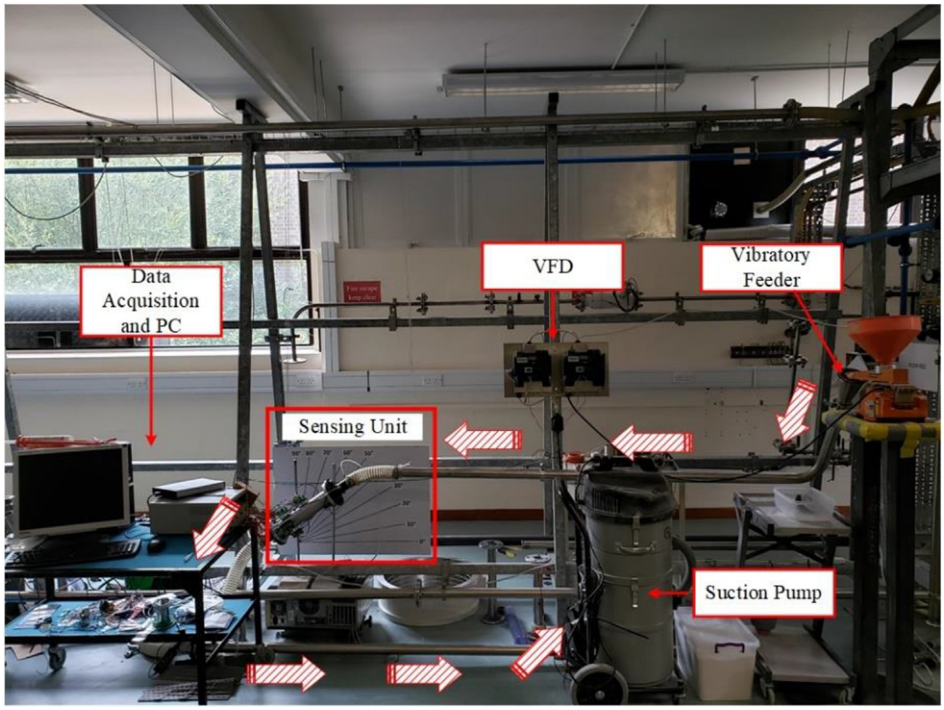

Fig. 6. Experimental setup.

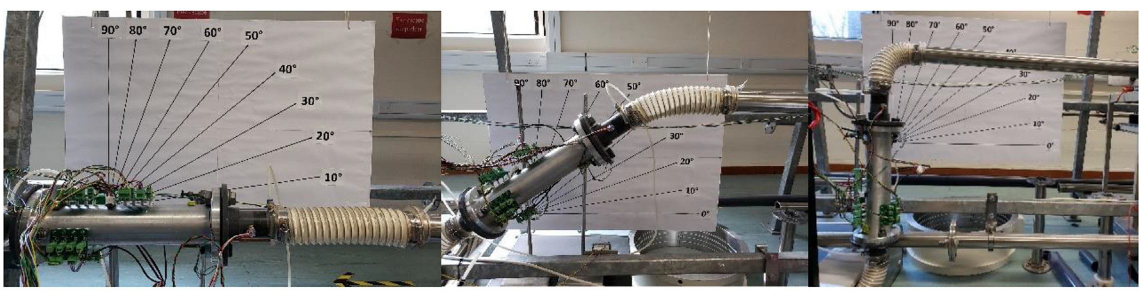

(a) (b) (c)

Fig. 7. Sensing unit in different orientations (a) 0° (b) 40° (c) 90°.

Table 1
Test conditions.

Test conditions	Value
Mass flow rate of particles (g/s)	3.2, 5.4, 7.7, 8.6, 11.3, 14.0, 17.6, 21.4, 25.7, 30.8, 35.8
Pipe angles (°)	0,10,20,30,40,50,60,70,80,90
Air velocity (m/s)	18
Temperature (°C)	23
Humidity (%)	46
Recording duration of each case (s)	30
Sampling rate (kHz)	20

The whole optimization process starts with the random initialization of the population that contains SVM model parameters. The fitness value of each set of model parameters is evaluated using the fitness function:

$$I_{fitness} = 9.4 \times 10^{10} e^{-11 \sum_{i=1}^{N_c} a_i err_i} + 0.3 \tag{1}$$

where N_c is the total number of mass flow rate conditions, err_i and a_i are the averaged relative error and scaling factor for the i^{th} mass flow rate condition, respectively. The fitness function produces the value based on the error between SVM predicted and actual results. The way each of the SVM model parameters moves towards optimal value in conjunction with fitness value in each iteration defines the relationship between noisy non-linear and the SVM parameters optimisation (Section 4.4).

Based on the intensity values of each firefly computed by the fitness function, each firefly makes a move towards the firefly of the highest intensity value. The position of i^{th} firefly that represents the value of k^{th} parameter of the model can be updated using Equation (2).

$$x_{ik} = x_{ik} + \beta_o e^{-\gamma \cdot r_{ij}} \left(x_{ik} - x_{jk}\right) + \alpha S_k \left(rand_{ik} - 0.5\right) \tag{2}$$

where.

x = Position of firefly
$rand$ = Random number generator
α = General scaling factor
β = Firefly attractiveness value
Υ = Media light absorption coefficient
S_k = Scaling factor of each parameter
$k = 1, 2, 3, \ldots, N_p$
N_p = Total number of parameters to be optimized

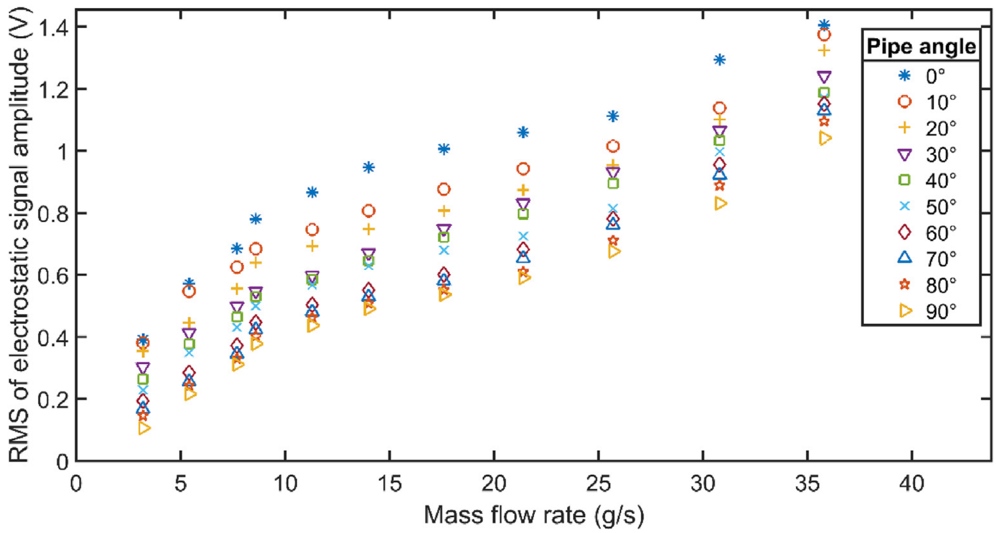

Fig. 8. Relationship between the RMS value of the signal from electrode E1 and mass flow rate of solids for particle velocity = 18 m/s, ambient temperature = 23 °C and RH = 46%.

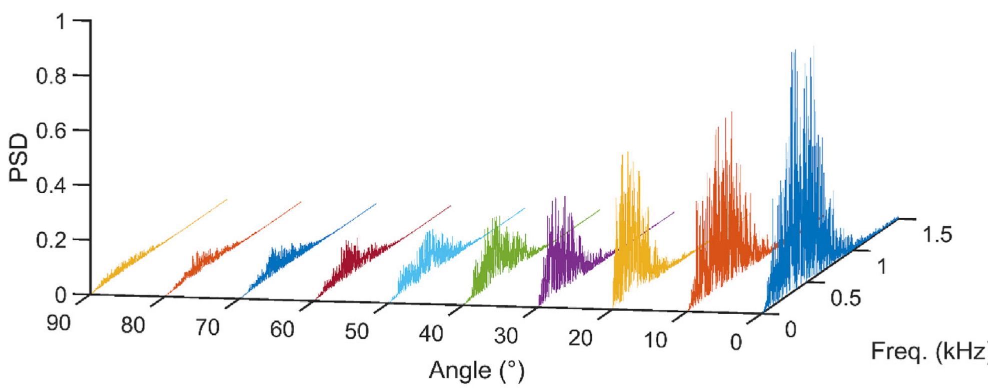

Fig. 9. PSD of the signal from electrode E1 in different pipe orientations for mass flow rate = 8.6 g/s, particle velocity = 18 m/s, ambient temperature = 23 °C and RH = 46%.

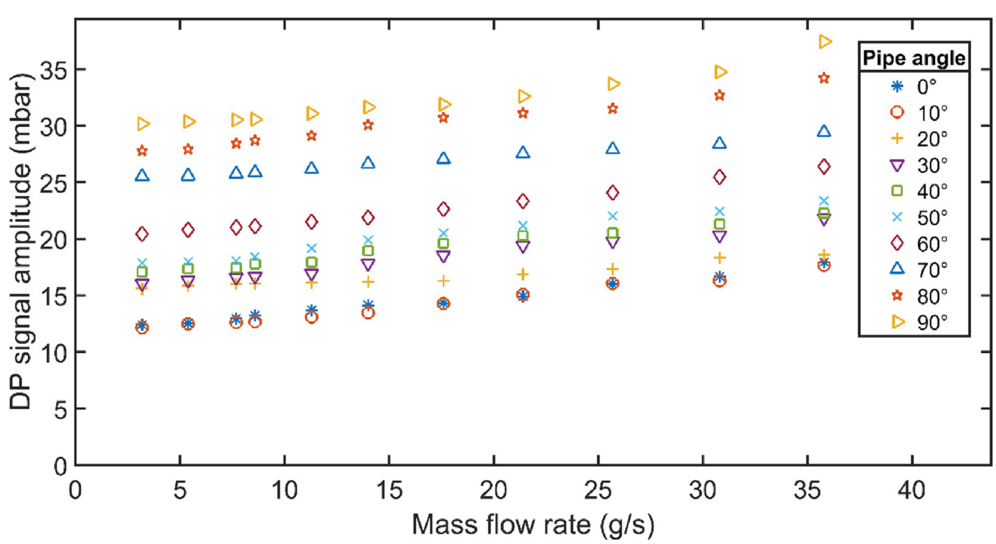

Fig. 10. Relationship between the DP signal and mass flow rate of solids.

$i,j = 1, 2, 3, \ldots, N_f$
N_f = Total number of fireflies
r_{ij} = Distance between fireflies

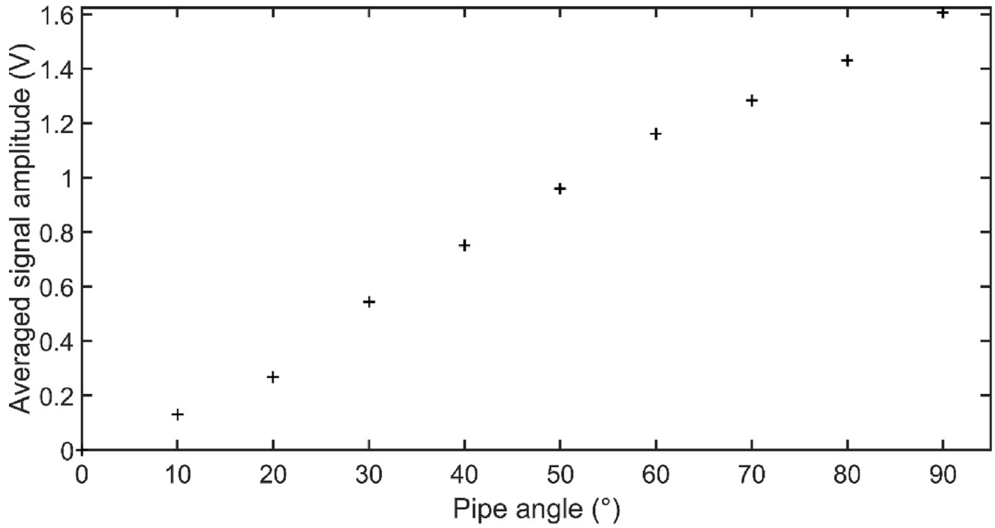

Fig. 11. Relationship between the output of the accelerometer and the pipe orientation.

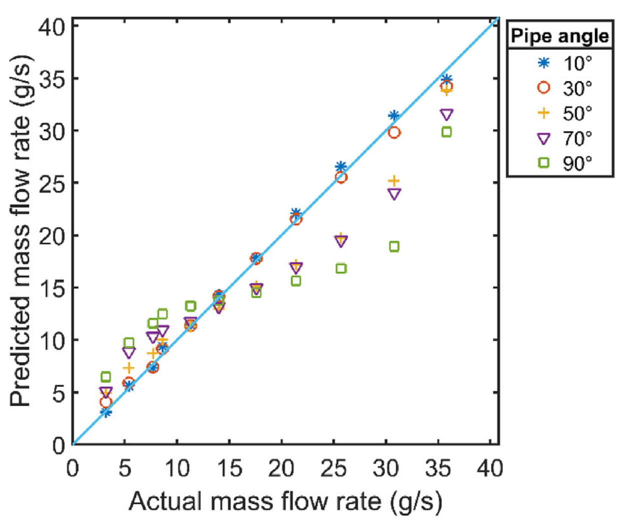

Fig. 12. Results from the conventional SVM model trained under horizontal pipe conditions.

where r_{ij} can be computed from,

$$r_{ij} = \sqrt{\sum_{k=1}^{N_p} (x_{ik} - x_{jk})^2} \tag{3}$$

where x_{ik} and x_{jk} are the positions of ith and jth fireflies which represent the values of kth parameter of the SVM model.

The whole algorithm keeps updating the parameters of the SVM model until either the iterations reach the maximum number of iterations or the intensity of the firefly reaches the threshold.

3. Experimental setup and test conditions

3.1. Experimental setup

Experiments were undertaken on a 50 mm bore laboratory-scale pneumatic conveying system to assess the performance of the proposed methodology. The pneumatic conveying system, as shown in Fig. 5, consists of a vibratory feeder, stainless steel pipe sections, and a suction pump. As the experiments were conducted in a laboratory environment, baking flour was used as test particles instead of pulverized coal for health and safety reasons. The sensing head was earthed along with the

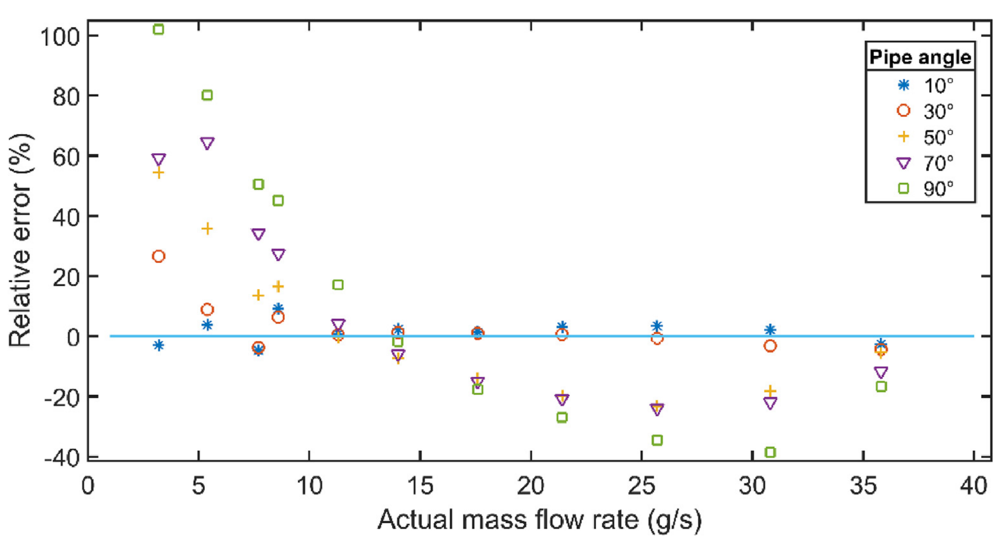

Fig. 13. Relative error of the conventional SVM model trained under horizontal pipe conditions.

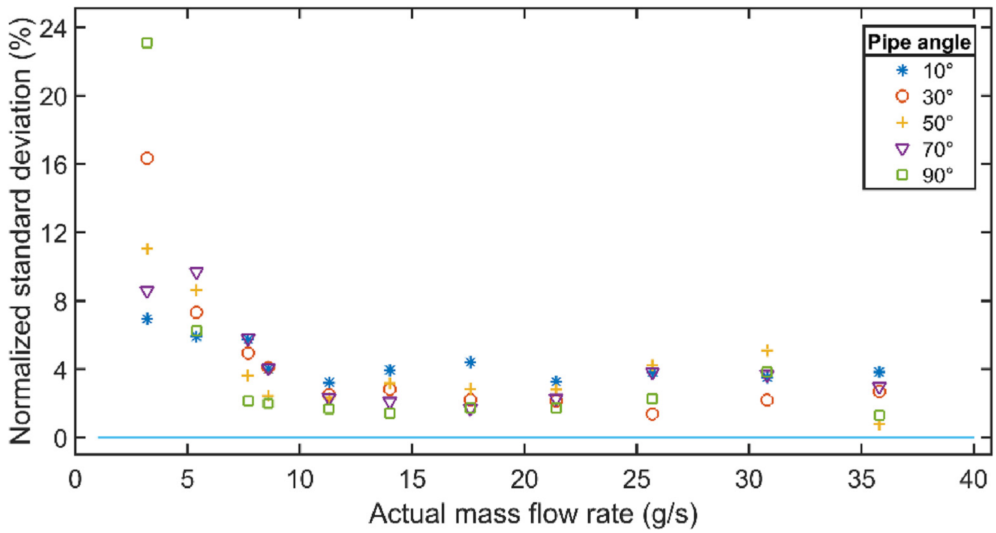

Fig. 14. Normalized STD of the conventional SVM model trained under horizontal pipe conditions.

Table 2
Dataset for training and testing.

Mass Flow Rate (g/s)	Training Angle (°)	Test Angle (°)
3.2, 5.4, 7.7, 8.6, 11.3, 14.0, 17.6, 21.4, 25.7, 30.8, 35.8	0	10
	20	30
	40	50
	60	70
	80	90

Table 3
Parameters of the conventional SVM model.

Parameter	Value
Kernel Scale	25
Delta Gradient Tolerance	0.005
Gap Tolerance	0.009
Epsilon	0.001
Number of Input Features	120

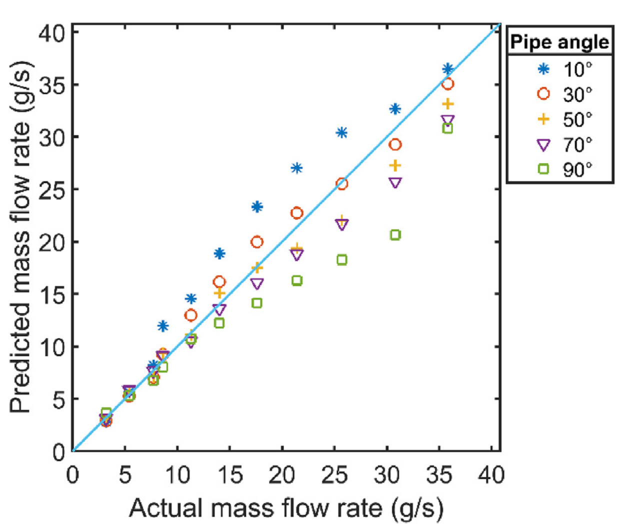

Fig. 15. Results from the conventional SVM model trained in different pipe orientations.

pipe sections to comply with relevant health and safety regulations. Solids were placed on the vibratory feeder and fed into the pipe with the generated vibration. The suction pump, in this case, was acting as a source of air to assist the particles to move in the counter-clockwise direction in the pneumatic flow loop. In order to change the mass flow rate conditions, the power of the vibratory feeder and suction pump was controlled by the variable frequency drive. All the sensor data was first conditioned and then acquired by a NI DAQ connecting to a computer. As illustrated in Fig. 6, the sensing unit was installed on the pneumatic pipe via flexible joints to make the sensing unit adjustable in any orientation. The flexible joints were only used to change the flow direction and the sensing head was firmly fixed on the rig frame during the experimental tests. Fig. 7 shows the orientation of the sensing unit when placed at the angle of 0°, 40° and 90°, respectively.

3.2. Test conditions

Experimental tests were conducted under the conditions outlined in Table 1. The test section was arranged in 10 different orientations. For each pipe angle, the mass flow rate of solids was adjusted from 3.2 g/s to 35.8 g/s. During the experiments, the ambient conditions were controlled at a temperature of 23 °C and humidity of 46%. For each test condition, the sensor signals were recorded for the duration of 30 s at the sampling rate of 20 kHz. These raw data will be analysed and processed further for training and testing of the SVM models (Section 4.3).

4. Results and discussion

4.1. Signals from the sensors

As the velocity of air remains constant throughout all the experiments, solids concentration increases with mass flow rate of solids. The signals from electrostatic sensors were collected in different mass flow rates in different pipe angles. The magnitude variations of the signals from the ring-shaped sensor E1 with the mass flow rate and pipe angle are depicted in Fig. 8. The RMS value is used to quantify the magnitude of each signal. The magnitude of each signal increases with the mass flow rate of solids. The placement of the sensing head at tilted orientations causes the solids to hit with the walls of the flexible joint, which can result in a possible reduction in particle's energy and charge magnitude. Therefore, at the same flow rate, the RMS value declines as the pipe angle increases. The rate of change of RMS value is higher in lower pipe angles. However, the rate of change decreases dramatically as the pipe is being tilted towards the vertical orientation. Furthermore, the possibility of

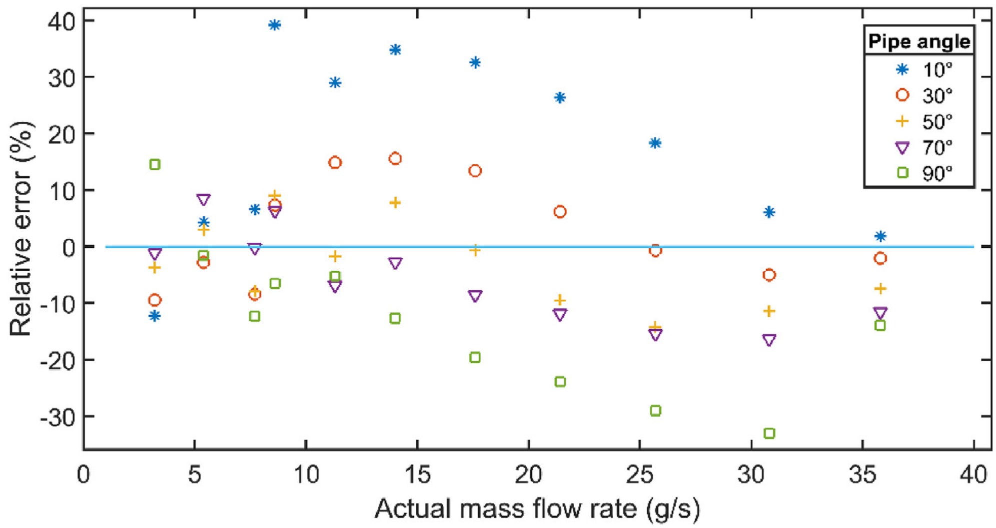

Fig. 16. Relative error of the conventional SVM model trained in different pipe orientations.

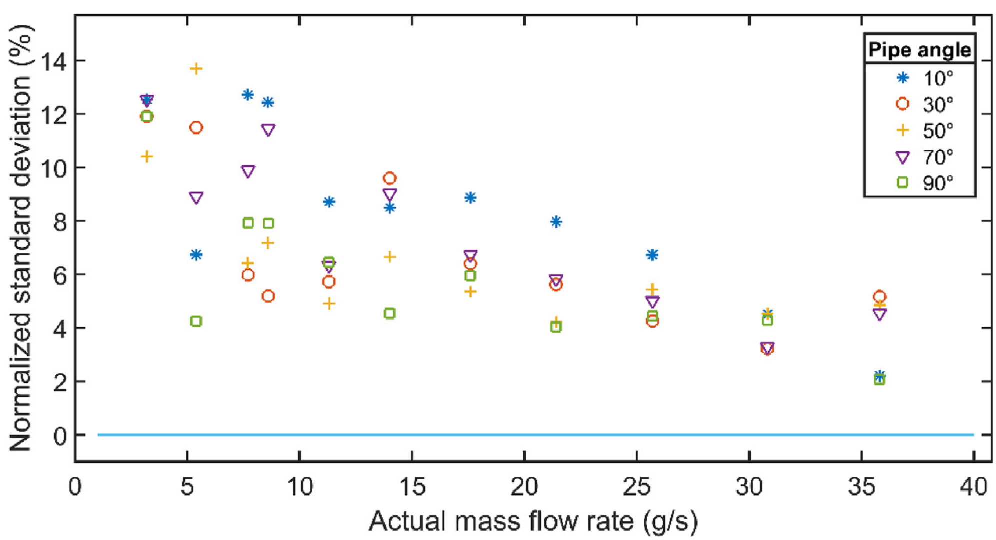

Fig. 17. Normalized STD of the conventional SVM model trained in different pipe orientations.

Table 4
Parameters of FA.

Parameter	Value
α	0.2
β	4
ϒ	0.01
S	[65, 0.3, 0.4, 1, 70]
N_p	300
N_{max}	500

solids to hit with the walls of flexible joint increases at higher mass flow rates hence a comparatively lower RMS charge value.

PSD of the electrostatic signals reflects the signal characteristics in the frequency domain. Fig. 9 shows the typical PSD spectrum of the signal which was collected from E1 at a constant mass flow rate of 8.6 g/s and different pipe angles. The amplitude of PSD is reduced as the pipe angle increases. PSD is a vital feature to comprehend the nature of variations in mass flow rate measurements in different pipe orientations.

The variations in the DP signal amplitude with the mass flow rate of solids in different pipe orientations are plotted in Fig. 10. With reference to Newton's second law of motion, the drop in line pressure is directly proportional to the solids-wall friction and solids gravity. The drop in line pressure increases with the mass flow rate of solids as a higher concentration of solids introduces more solids-wall friction and hence more energy is required to convey the solids from the upstream to the downstream of the spoolpiece. The velocity of conveying air was kept constant throughout the experiments, so the increasing mass flow rate of solids entails rising solids concentration and hence higher pressure drop. Furthermore, for a given mass flow rate of solids, a rising trend is observed in differential pressure with an increasing pipe angle because of the increasing gravitational effect on solids.

RMS of electrostatic signals is a key feature in the time domain, indicating the amplitude of electrostatic signals, which is closely related to solids velocity and concentration. PSD is a feature in the frequency domain, providing complementary information about the two-phase flow. DP signal amplitude is directly related to the velocity of the mixture flow and solids concentration. In view of their physical meanings, they are three important, independent and complementary features to infer the mass flow rate of solids.

The purpose of installing an accelerometer on the sensing unit is to collect the information about the pipe orientation. Therefore, the signal output from this sensor has nothing to do with the mass flow rate of solids

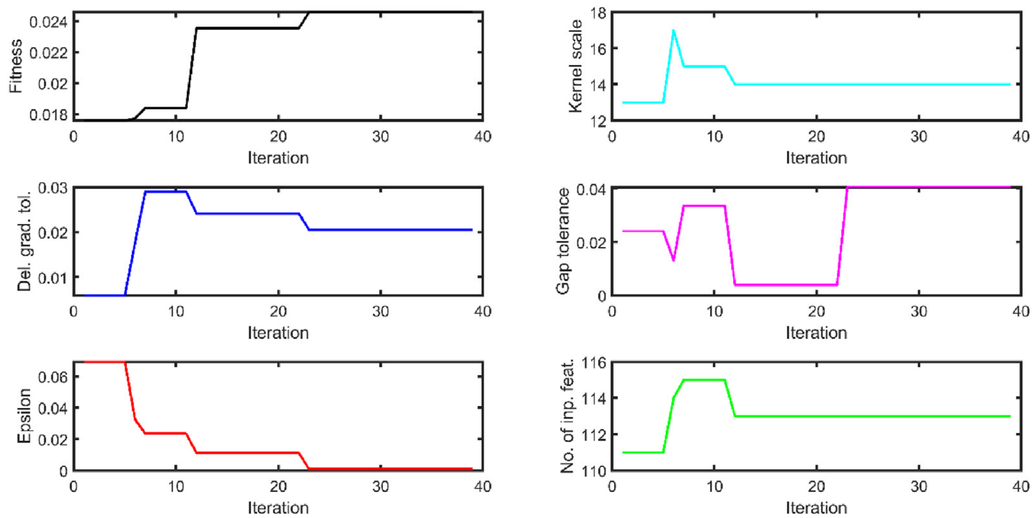

Fig. 18. Performance of the FA

Table 5
Optimized parameters of the SVM model.

Parameter	Value
Kernel Scale	9
Delta Gradient Tolerance	0.0481
Gap Tolerance	0.0079
Epsilon	0.1469
Number of Input Features	93

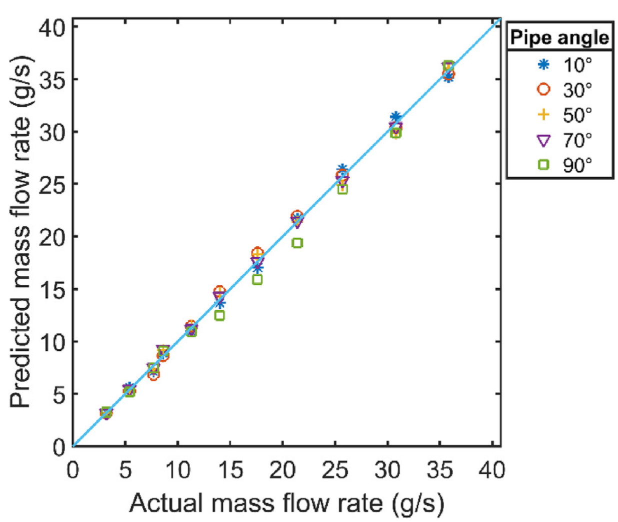

Fig. 19. Results from the optimized SVM model trained in different pipe orientations.

but the orientation of the pipe. Fig. 11 shows the averaged value of the post-processed signal from the accelerometer in different pipe orientations.

4.2. Conventional SVM model trained under horizontal pipe conditions

The conventional SVM model was trained with the dataset and parameters used in the previous study [12]. Training data were collected when the sensing unit was installed at a fixed angle of 0°. However, testing was done with the data collected in different angles (10°, 30°, 50°, 70° and 90°). Fig. 12 shows the predicted mass flow rate from the conventional SVM model at eleven different mass flow rate conditions. The straight line shows the scenario where the predicted measurements are ideally assumed to be the same as a reference. A significant amount of variation from the ideal straight line can be seen in the predicted measurements, especially at the lower mass flow rate and larger pipe angles. This is due to the fact that the movement of sensing head towards vertical orientation introduces the change in flow regime and result in different characteristics in sensor signals. Because of the limitation of the generalisation ability of data-driven models, the SVM model developed based on the data from a single pipe orientation cannot well predict the mass flow rate at other pipe orientations.

Fig. 13 shows that the relative error is moderately higher under the lower mass flow rate conditions and reduces significantly with the mass flow rate of solids. This is caused by the flow regime effects in the pneumatic conveying pipe. Flow regime stays homogenous at a lower mass flow rate due to the uniform distribution of particles. The higher ratio of particles in uniform distribution loses the energy after hitting with the curved wall of the flexible joint and hence causes the measurement error. As the mass flow rate increases, the flow regime becomes stratified due to the reason that at constant velocity and higher solids concentration, most of the particles travel in the lower part of the pipe. The particles which are moving along the lower part of the pipe can easily pass by the curved wall of the flexible joint and hence lower measurement error due to the preservation of particles energy. Repeatability of these measurements is also observed by calculating the normalized standard deviation, as shown in Fig. 14. Loss of particles energy at lower mass flow rate conditions produces inconsistent and less reliable sensor data compared to the higher mass flow rate conditions which affect the repeatability of the measurements accordingly. Variations in the predicted mass flow measurement demonstrate the impact of the pipe orientation on the mass flow rate measurement.

4.3. Conventional SVM model trained in different pipe orientations

As the orientation of the sensing unit does have an impact on the characteristics of sensor signals and affect the performance of the data-driven model, sensor signals in different orientations are added to the training data to make the model adaptive to the orientation of the sensing unit. The experimental test conditions for training data and test data are summarized in Table 2. A new model based on conventional SVM was trained in five different angles and eleven mass flow rate conditions. However, the test data were collected completely different from the conditions of training data to analyse the generalization capability of the model. In the training process, the selection of useful features and SVM model parameters were manually determined by trial and error method.

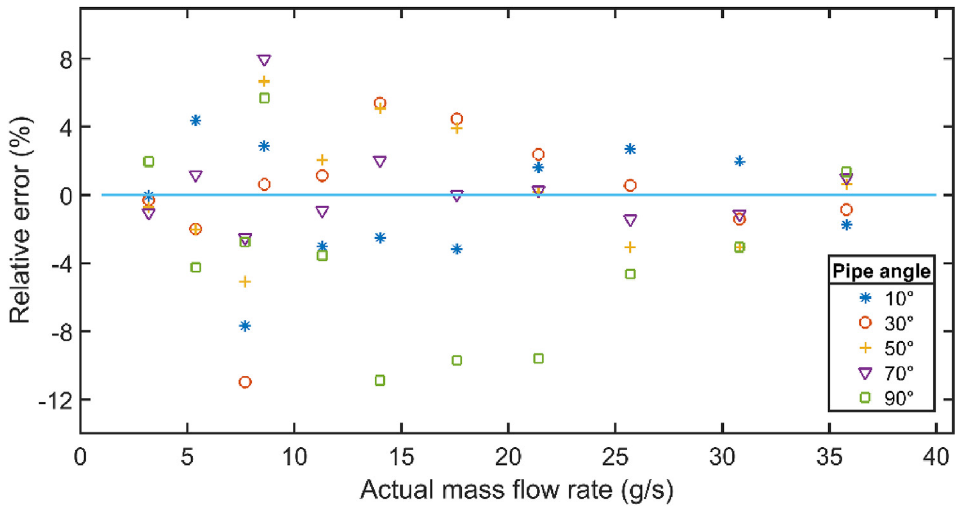

Fig. 20. Relative error of the optimized SVM model trained in different pipe orientations.

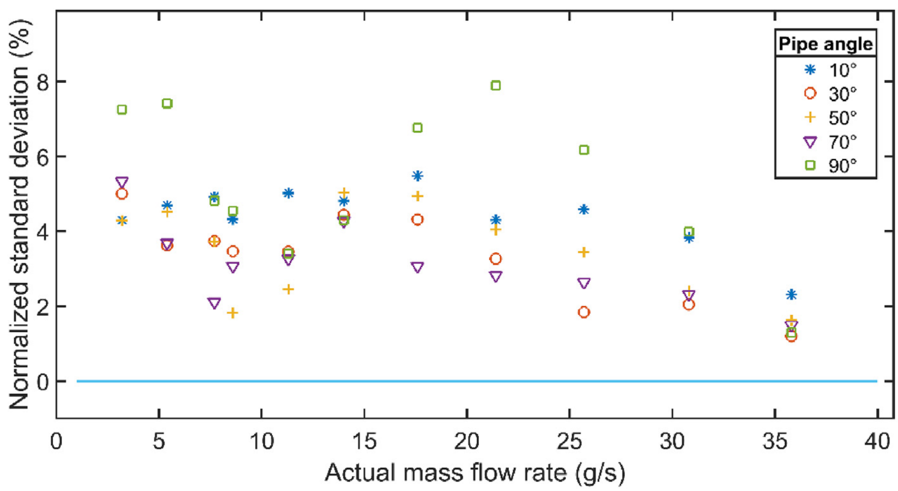

Fig. 21. Normalized STD of the optimized SVM model trained in different pipe orientations.

Table 3 shows the parameters used in the conventional SVM model.

Fig. 15 shows the predicted measurements under eleven mass flow rate conditions in five different angles of the sensing unit. The proximity of measured mass flow rate values with the ideal straight line demonstrates the effectiveness of compensation of pipe orientation. The relative error of the predicted measurements from conventional SVM trained in different pipe orientations is shown in Fig. 16. In comparison with the results in Fig. 13, the relative error is significantly reduced to within ±40%. Likewise, the repeatability of the measurements has also been improved and the maximum normalized standard deviation is reduced down to 14% as shown in Fig. 17.

4.4. Optimised SVM model trained in different pipe orientations

In this section the SVM model is trained and tested using the data outlined in Table 2. As the performance of the SVM model is also influenced by the learning parameters of the model, therefore FA is applied to find the optimal parameters in the SVM model. The FA has created 300 elements in the entire population where each element contains all the tuning parameters of the SVM model, as mentioned in Section 2.3. The FA has calculated the fitness value of each element in the population using Equation (1) to analyze the performance. The higher fitness value of an element indicates that the element is closer to the optimal value of the model parameters. Based on the selection of the best element, FA then keeps creating a new population around that best element of the previous population. FA has generated the optimized SVM parameters based on the best element of the final population when the algorithm is terminated. The whole algorithm terminates when either the accuracy of the SVM model reaches the desired level or if there are no significant changes observed in the accuracy of the SVM model for a specific number of iterations. In this case, FA has converged to the optimized solution in 32 iterations by using the parameters, as listed in Table 4. The parameters for FA are chosen through trial and error by limiting the maximum number of iterations (N_{max}) to 500.

The performance of the FA in each iteration including the value of fitness function and the parameters of the SVM model, including kernel scale, delta gradient tolerance, gap tolerance, epsilon, and the number of input features can be seen in Fig. 18. Stability in the fitness value after 16th iteration shows that the FA has approached to its saturation state by giving the best suitable parameters mentioned in Table 5.

Fig. 19 shows the mass flow rate measurements from the optimized SVM model. The very close proximity of measured points to the ideal straight line shows the effectiveness of the proposed model. A deep-down analysis is undertaken based on the relative error between measured and the reference mass flow rate conditions shown in Fig. 20. Measurements taken at the angle of 10 and 30° have a relative error within the range of

±12% for lower mass flow rate conditions and it reduces down to ±4% for higher mass flow rates. At the angle of 50°, relative error fluctuates between ±7% at lower mass flow rate conditions but it stays reasonably low at higher mass flow rate conditions. Measurements, taken at 70 and 90°, exhibit the relative error that is heavily dispersed between ±12% because the orientation of the sensing unit is approaching towards vertical orientation and the particles are partially disturbed by the walls of the flexible joint. As shown in Fig. 21, the repeatability of the measurements is improved and the normalized standard deviation is within 8%.

5. Conclusion

A multi-modal sensing unit, including ring and arc-shaped electrostatic sensors, a DP transducer and an accelerometer, in conjunction with optimized SVM model, has been proposed to measure the mass flow rate of solids in different pipe orientations. Experimental tests were conducted with mass flow rate of solids ranging from 3.2 g/s to 35.8 g/s in a pipe angle from 0° to 90°. It has been observed that the RMS magnitude of the signal and corresponding PSD reduce down as the pipe moves from the horizontal to vertical orientation. The performance of the conventional SVM model trained under horizontal pipe conditions is unsatisfactory due to the limited generalization ability and lack of flow information in different pipe orientations. By training the SVM model in different pipe orientations, the relative error has been reduced from ±100% to ±40%. As the firefly optimization algorithm has been used to determine the parameters of the SVM model and the number of input features, the relative error has been reduced to ±12% with the maximum normalized standard deviation of 8%. The results have demonstrated the effectiveness of the proposed methodology to measure the mass flow rate of solids in an air suspension in different pipe orientations.

CRediT authorship contribution statement

Faisal Abbas: Methodology, Software, Validation, Writing - original draft. **Lijuan Wang:** Methodology, Software, Supervision, Writing - review & editing. **Yong Yan:** Conceptualization, Methodology, Supervision, Writing - review & editing.

Declaration of competing interest

The authors declare that they have no known competing financial interests or personal relationships that could have appeared to influence the work reported in this paper.

References

[1] X. Qian, Y. Yan, X. Huang, Y. Hu, Measurement of the mass flow and velocity distributions of pulverized fuel in primary air pipes using electrostatic sensing techniques, IEEE Trans. Instrum. Meas. 66 (5) (May 2017) 944–952.

[2] N.A. Zulkiflli, S. Ibrahim, M.H.F. Rahiman, J. Pusppanathan, R.A. Rahim, K.S. Tee, F.A. Phang, N.D. Nawi, N.M.N. Ayob, Ultrasound tomography hardware system for multiphase flow imaging, in: 2019 IEEE International Conference on Signal and Image Processing Applications (ICSIPA), Kuala Lumpur, Malaysia,, Sep. 2019, pp. 264–268.

[3] X. Wang, Y. Hu, H. Hu, L. Li, Evaluation of the performance of capacitance sensor for concentration measurement of gas/solid particles flow by coupled fields, IEEE Sensor. J. 17 (12) (June 2017) 3754–3764.

[4] N.O. Mahony, T. Murphy, K. Panduru, D. Riordan, J. Walsh, Acoustic and optical sensing configurations for bulk solids mass flow measurements, in: 2016 10th International Conference On Sensing Technology (ICST), Nanjing, China, 2016, pp. 1–6.

[5] X. Qian, Y. Yan, L. Wang, J. Shao, An integrated multi-channel electrostatic sensing and digital imaging system for the on-line measurement of biomass-coal particles in fuel injection pipelines, Fuel 151 (Jul. 2015) 2–10.

[6] A. Bilgic, J. Kunze, V. Stegemann, J. Hogendoorn, M. Zoeteweij, Multiphase flow metering with nuclear magnetic resonance spectroscopy, in: In *AMA Conferences*, May 2015, pp. 292–297. Nurnberg, Germany.

[7] Y. Yan, L. Wang, T. Wang, X. Wang, Y. Hu, Q. Duan, Application of soft computing techniques to multiphase flow measurement: a review, Flow Meas. Instrum. 60 (Apr. 2018) 30–43.

[8] L. Wang, J. Liu, Y. Yan, X. Wang, T. Wang, Gas-liquid two-phase flow measurement using coriolis flowmeters incorporating artificial neural network, support vector machine and genetic programming algorithms, IEEE Trans. Instrum. Meas. 66 (5) (May 2017) 852–868.

[9] X. Wang, H. Hu, A. Zhang, Concentration measurement of three-phase flow based on multi-sensor data fusion using adaptive fuzzy inference system, Flow Meas. Instrum. 39 (Jun. 2014) 1–8.

[10] H. Hu, J. Dong, J. Zhang, Y. Cheng, T. Xu, Identification of gas/solid two-phase flow regimes using electrostatic sensors and neural-network techniques, Flow Meas. Instrum. 22 (5) (Oct. 2011) 482–487.

[11] Y. Yan, L. Xu, P. Lee, Mass flow measurement of fine particles in a pneumatic suspension using electrostatic sensing and neural network techniques, IEEE Trans. Instrum. Meas. 55 (6) (Dec. 2006) 2330–2334.

[12] F. Abbas, Y. Yan, L. Wang, Mass flow measurement of pneumatically conveyed solids through multi-modal sensing and machine learning, in: 2020 IEEE International Instrumentation and Measurement Technology Conference (I2MTC), Dubrovnik, Croatia, May 2020.

[13] X.-Q. Bian, L. Zhang, Z.-M. Du, J. Chen, J.-Y. Zhang, Prediction of sulfur solubility in supercritical sour gases using grey wolf optimizer-based support vector machine, J. Mol. Liq. 261 (Jul. 2018) 431–438.

[14] E. Tuba, I. Strumberger, T. Bezdan, N. Bacanin, M. Tuba, Classification and feature selection method for medical datasets by brain storm optimization algorithm and support vector machine, Procedia Comput. Sci. 162 (Nov. 2019) 307–315.

[15] N.A. Hitam, A.R. Ismail, F. Saeed, An optimized support vector machine (svm) based on particle swarm optimization (pso) for cryptocurrency forecasting, Procedia Comput. Sci. 163 (Dec. 2019) 427–433.

[16] M. Rajalakshmi, S. Jeyadevi, C. Karthik, "An application of hybrid firefly and pso with support vector regression for modelling a clarifier process in sugar industry, in: *2018 National Power Engineering Conference (NPEC)*, Madurai, India, Oct. 2018, pp. 1–10.

[17] S. Agarwal, A.P. Singh, N. Anand, Evaluation performance study of firefly algorithm, particle swarm optimization and artificial bee colony algorithm for non-linear mathematical optimization functions, in: *2013 Fourth International Conference On Computing, Communications And Networking Technologies (ICCCNT)*, Tiruchengode, India, Jul. 2013, pp. 1–8.

[18] N.M. Tripathi, D. Portnikov, A. Levy, H. Kalman, Bend pressure drop in horizontal and vertical dilute phase pneumatic conveying systems, Chem. Eng. Sci. 209 (Dec. 2019) 115228.

[19] S. Khurram, J.-H. Choi, Y. Won, A.-R. Jeong, H.-J. Ryu, Relationship between solid flow rate and pressure drop in the riser of a pressurized circulating fluidized bed, J. Chem. Eng. Jpn. 49 (01 2016) 595–601.

[20] G.J. Bowden, G.C. Dandy, H.R. Maier, Input determination for neural network models in water resources applications, J. Hydrol. 301 (1) (Jan. 2005) 75–92.

[21] N. Guenther, M. Schonlau, Support vector machines, STATA J. 16 (4) (May 2016) 917–937.

[22] X.-S. Yang, Firefly algorithms for multimodal optimization, in: " Stochastic Algorithms: Foundations And Applications, 2009, pp. 169–178. Berlin, Heidelberg, Mar.